Investigation on four-port mono-capacitor circuit with high-pass negative group delay behavior

Sofia Fenni, Fayrouz Haddad, Antonio Jaomiary, Samar Yazdani, Frank Elliot Sahoa, Lucius Ramifidisoa, Mathieu Guerin, Wenceslas Rahajandraibe, Blaise Ravelo

Investigation on four-port mono-capacitor circuit with high-pass negative group delay behavior

Sofia Fenni[1], Fayrouz Haddad[1], Antonio Jaomiary[2], Samar S. Yazdani[3],
Frank Elliot Sahoa[4], Lucius Ramifidisoa[2], Mathieu Guerin[7], Wenceslas Rahajandraibe[1], and Blaise Ravelo[5]

[1] Aix-Marseille University, CNRS, University of Toulon, IM2NP UMR7334, Marseille, France
[2] Ecole Normale Supérieure pour l'Enseignement Technique (ENSET), University of Antsiranana,
BP O, Antsiranana 201, Madagascar
[3] Bahria University Karachi Campus, Software Engineering Department, Karachi, Pakistan
[4] Laboratoire de Physique Nucléaire et Physique de l'Environnement (LPNPE),
Univ. d'Antananarivo - Madagascar
[5] Nanjing University of Information Science & Technology (NUIST), Nanjing, Jiangsu 210044, China
E-mail: sofia.fenni@gmail.com, fayrouz.haddad@im2np.fr, jaomiaryantonio@yahoo.fr, ssamaryazdani@gmail.com,
sfrankelliot@gmail.com, ramifidisoa@yahoo.fr, mathieu.guerin@im2np.fr, wenceslas.rahajandraibe@im2np.fr,
blaise.ravelo@yahoo.fr
Corresponding author: jaomiaryantonio@yahoo.fr

Abstract: Most of the negative group delay (NGD) circuit recent investigation were focused on the classes of low-pass and bandpass categories. Few research works are currently available in the literature on the typical high-pass (HP) NGD function. This paper introduces an original HP-NGD circuit theory of four-port passive topology constituted by a single lumped capacitor. The S-matrix equivalent model of the innovative topology is established from the admittance matrix. Then, the basic frequency analytical responses are expressed. Then, the GD model is derived in function of the capacitor. It was found analytically that the four-port mono-capacitor passive circuit is susceptible to behave originally as an unfamiliar HP-NGD function. An innovative HP-NGD analysis is explored in addition to the expression of synthesis design equation in function of the expected NGD cut-off frequency which is linked to NGD optimal value. The validity of the established HP-NGD circuit theory is verified with a proof of concept (POC). As expected, the HP-NGD behavior showing a good correlation between analytical model and simulation is obtained.

Keywords: Mono-capacitor circuit, four-port topology, high-pass (HP) negative group delay (NGD), NGD function, NGD analysis, NGD specifications, S-matrix modelling.

1. INTRODUCTION

In addition to the noise, the delay effect is one of the most penalizing effect which limits the electronic and communication system performances [1-3]. An unfamiliar negative group delay (NGD) equalization and neutralization solution against the delay effect was recently initiated [4-5]. The NGD solution is also promising for the distorted signal reconstruction [6]. The NGD function was more generally suggested to compensate for communication system delay [7], enhanced bandwidth feedback microwave amplifiers [8-9] and design of reconfigurable series feed network for squint-free antenna beamforming [10]. However, because of particularly counterintuitive NGD effect, further research work is needed to open the NGD circuit design to non-specialist electronic engineers.

The existence of negative group delay (NGD) effect is one of most curious questions of physicists in the twentieth century. The unfamiliar NGD effect was observed in first time based on optical experimentation with negative group velocity (NGV) media [11-12]. Diverse unfamiliar NGD investigations with optical system were conducted by showing counterintuitive superluminal pulse propagation [13-14]. In addition, for further physical understanding, theoretical study of NGD effect was also developed via transfer function elaboration [13-14]. The curious question about the NGD function existence in the electronic circuits attracted the attention of some design researchers [15-20]. Therefore, theoretical and experimental studies of low frequency (LF) NGD circuits were performed by using R, L, C and operational amplifier [15-16]. The extraordinary experimentation of smoothed pulse signal in millisecond time-advance and in superluminal propagation was performed [17-19]. It was emphasized that the NGD effect does not contradict the causality principle [15-16].

Despite the notable limitation reported on the NGD properties [20], the NGD effect existence in microwave frequencies was an open question [21-32]. Remarkable NGD microwave passive circuits were designed in early 2000s from metamaterial based negative refractive index and split ring resonator structures [21-24]. However, the metamaterial based NGD passive circuits are significantly lossy and limit the opportunity of their applications. Emphatically, intensive research works were made on low attenuation loss NGD passive circuits last two decades [25-30]. Nevertheless, the diversity of NGD circuit structures leads to wonder about the general topologies of the unfamiliar electronic function. Such a question motivates to initiate a fundamental circuit theory of NGD function inspired from filter function [31].

The innovative concept of low-pass (LP) [6,31] and bandpass (BP) [31-33] NGD circuit classification was established. Furthermore, we are constantly looking for the simplest NGD topologies by using resistive-capacitive network [6], resistorless lumped network [32] and capacitive-network [33]. In difference to the all existing NGD research work, we are developing a circuit theory of mono-capacitor and extremely simple topology in the present paper.

2. S-PARAMETER MODELLING OF THE MONO-CAPACITOR NGD TOPOLOGY

The present section describes the topological identification of the mono-capacitor NGD circuit. For the better understanding about the unfamiliar NGD aspect, the basic function will be defined. Then, the S-parameter model will be exploited to elaborate the NGD class identification, and analysis.

2.1. Topological description

We are expecting a first order NGD topology. Therefore, must be composed of at least a reactive component [31]. Accordingly, we can choose the impedance Z a first order element. Before the NGD topological identification, we can consider the four-port H-shape circuit shown by Fig. 1. By denoting the Laplace variable, s, the proposed circuit can be assumed to be composed of central element represented by an impedance, $Z(s)=1/(Cs)$ and four lumped identical resistances, R. To analyze the circuit, each port $n=\{1,2,3,4\}$ is connected to voltage source V_n with the input current I_n. By using the Kirchhoff voltage and current laws (KVL and KCL), we can write the following relathinoships:

$$V_1(s)-V_4(s)=RI_1(s)-RI_4(s) \tag{1}$$

$$V_2(s)-V_3(s)=RI_2(s)-RI_3(s) \tag{2}$$

$$V_1(s)-V_2(s)=RI_1(s)+Z(s)\left[I_1(s)+I_4(s)\right]-RI_2(s) \tag{3}$$

$$I_1(s)+I_2(s)+I_3(s)+I_4(s)=0 \tag{4}$$

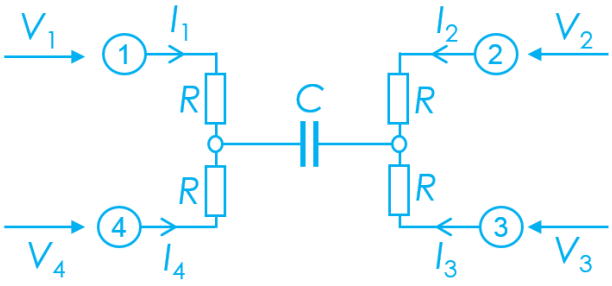

Figure 1: *R* and *Z* impedance based four-port circuit.

These KVL and KCL will serve in the following paragraph to establish the admittance matrix model of our four-port circuit.

2.2. Admittance matrix modelling

The matrix equivalent of these four linear relations is expressed as:

$$\left[\Gamma\right]\times\begin{bmatrix}V_1(s)\\V_2(s)\\V_3(s)\\V_4(s)\end{bmatrix}=\left[\Omega(s)\right]\times\begin{bmatrix}I_1(s)\\I_2(s)\\I_3(s)\\I_4(s)\end{bmatrix} \tag{5}$$

with:

$$\left[\Gamma\right]=\begin{bmatrix}1&0&0&-1\\0&1&-1&0\\1&-1&0&0\\0&0&0&0\end{bmatrix} \tag{6}$$

$$[\Omega(s)]=\begin{bmatrix} R & 0 & 0 & R \\ 0 & R & -R & 0 \\ R+Z(s) & -R & 0 & Z(s) \\ 1 & 1 & 1 & 1 \end{bmatrix}. \quad (7)$$

According to the system theory, the admittance matrix is linked to the input voltage and access current by the matrix relationship:

$$\begin{bmatrix} I_1(s) \\ I_2(s) \\ I_3(s) \\ I_4(s) \end{bmatrix}=[Y(s)]\times\begin{bmatrix} V_1(s) \\ V_2(s) \\ V_3(s) \\ V_4(s) \end{bmatrix}. \quad (8)$$

By algebraic identification between equation (5) and equation (8), we established that the admittance matrix of our four-port network:

$$[Y(s)]=[\Omega(s)]\times[\Gamma]. \quad (9)$$

Consequently, we have:

$$[Y(s)]=\frac{\begin{bmatrix} 3R+2Z(s) & -R & -R & -R-2Z(s) \\ -R & 3R+2Z(s) & -R-2Z(s) & -R \\ -R & -R-2Z(s) & 3R+2Z(s) & -R \\ -R-2Z(s) & -R & -R & 3R+2Z(s) \end{bmatrix}}{4R[R+Z(s)]} \quad (10)$$

This admittance matrix will be exploited in the next subsection to determine the S-matrix of the NGD circuit.

2.3. S-matrix modelling

Let us consider the four-port black box introduced in Fig. 2. The S-matrix equivalent model can be generally denoted by:

$$[S(s)]=\begin{bmatrix} S_{11}(s) & S_{12}(s) & S_{13}(s) & S_{14}(s) \\ S_{21}(s) & S_{22}(s) & S_{23}(s) & S_{24}(s) \\ S_{31}(s) & S_{32}(s) & S_{33}(s) & S_{34}(s) \\ S_{41}(s) & S_{42}(s) & S_{43}(s) & S_{44}(s) \end{bmatrix} \quad (11)$$

This S-matrix is referenced by the access port impedance R_0=50 Ω.

Figure 2: Four-port S-parameter model.

According to the S-matrix theory, we have the Y-to-S matrix transform:

$$[S(s)] = \{[Id_4] - R_0[Y(s)]\} \times \{[Id_4] + R_0[Y(s)]\}^{-1} \tag{12}$$

with the 4-D identity matrix:

$$[Id_4] = \begin{bmatrix} 1 & 0 & 0 & 0 \\ 0 & 1 & 0 & 0 \\ 0 & 0 & 1 & 0 \\ 0 & 0 & 0 & 1 \end{bmatrix} \tag{13}$$

Substituting the admittance matrix given in equation (10) into relationship (12), we have the following symmetric matrix:

$$[S(s)] = \frac{\begin{bmatrix} N_1(s) & N_2(s) & N_2(s) & N_3(s) \\ N_2(s) & N_1(s) & N_3(s) & N_2(s) \\ N_2(s) & N_3(s) & N_1(s) & N_2(s) \\ N_3(s) & N_2(s) & N_2(s) & N_1(s) \end{bmatrix}}{D(s)} \tag{14}$$

where:

$$\begin{cases} N_1(s) = R[2R + R_0 + 2Z(s)] - R_0^2 \\ N_2(s) = R_0(R_0 + R) \\ N_3(s) = R_0[R_0 + R + 2Z(s)] \\ D(s) = 2(R_0 + R)[R + R_0 + Z(s)] \end{cases}. \tag{15}$$

From this S-matrix, the NGD topological analysis can be elaborated.

2.4. NGD topological identification

By the reason of simplicity, let us take R=0 or replaced by short-circuited branches. Therefore, we have the reduced four-port topology depicted by Fig. 3 which is constituted only by a capacitive component C. The associated S-matrix given by equation (14) is composed of elements of written as:

$$\begin{cases} N_1(s) = -R_0 \\ N_2(s) = R_0 \\ N_3(s) = R_0 + 2Z(s) \\ D(s) = 2[R_0 + Z(s)] \end{cases}. \tag{16}$$

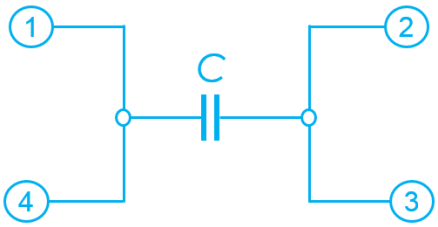

Figure 3: Mono-capacitor four-port circuit.

Therefore, we have a possibility to generate NGD function between ports ❶-❹ and ❷-❸ by means of:

- Reflection coefficients:

$$S_{nn}(s)=\frac{N_1(s)}{D(s)}=\frac{-R_0}{2\left[R_0+Z(s)\right]} \tag{17}$$

- Transmission coefficients:

$$T(s)=S_{41,32}(s)=\frac{N_3(s)}{D(s)}=\frac{R_0+2Z(s)}{2\left[R_0+Z(s)\right]}. \tag{18}$$

By choosing the impedance as a capacitor component, $Z(s)=1/(Cs)$, the previous coefficients can be simplified as transfer functions:

$$S_{nn}(s)=\frac{-R_0Cs}{2(1+R_0Cs)} \tag{19}$$

$$T_L(s)=\frac{2+R_0Cs}{2(1+R_0Cs)}. \tag{20}$$

The NGD analysis of this transfer function will be explored in the following section.

3. NGD ANALYSIS OF THE IDENTIFIED PASSIVE TOPOLOGY

The NGD analysis of the mono-capacitor based circuit topology will be explored theoretically in the present section. The expressions of the previously introduced NGD characteristics will be expressed in function of the capacitor component.

3.1 Basic frequency responses needed for the NGD analysis

The NGD study of a circuit depends essentially on the analysis of transmission coefficient. By taking the Laplace variable versus angular frequency, $s=j\omega$, the transmission coefficient (with integer subscript, $m\neq n$) can be expressed as:

$$T(j\omega)=S_{mn}(j\omega). \tag{21}$$

The basic elements to explore this response are transmittance, $T(\omega)$, and phase, $\varphi(\omega)$ which are given by respectively:

$$T(\omega) = \left|T(j\omega)\right| \tag{22}$$

$$\varphi(\omega) = \arg\left[T(j\omega)\right]. \tag{23}$$

We can derive from this last expression, according to circuit theory, the GD defined by the following equation:

$$GD(\omega) = -\frac{\partial\varphi(\omega)}{\partial\omega}. \tag{24}$$

Knowing these fundamental elements, we can explore the unfamiliar NGD response. The basic characteristics of this response can be introduced as described in the following paragraph.

3.2 HP-NGD ideal specifications

The unfamiliar HP-NGD analysis of our four-port mono-capacitor passive topology must be performed with respect to specific parameters linked to the frequency responses. In this case of study, in difference to most of classical electronic circuit, the main parameters of the characterization are essentially the GD and the magnitude. Subsequently, Fig. 4(a) and Fig. 4(b) introduce ideal plots associated the GD and transmission coefficient magnitude.

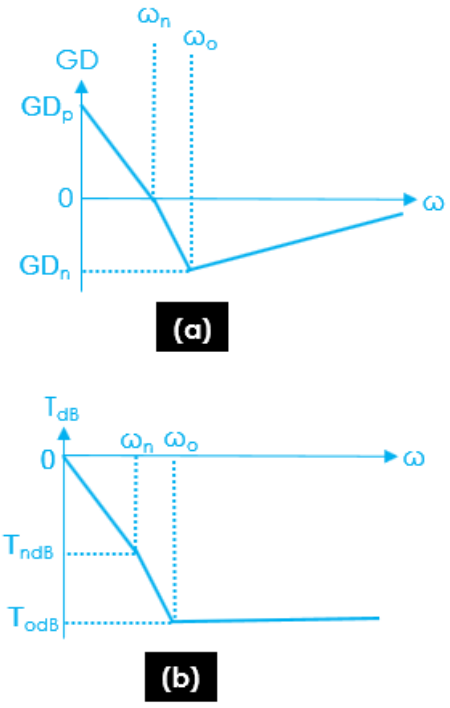

Figure 4: NGD specifications: (a) GD and (b) transmission coefficient magnitude.

We remind that if GD_0<0, the circuit can be classified as LP-NGD topology. To operate as a HP NGD circuit, the LF GD value defined in equation (24) is equal to:

$$GD(\omega \approx 0) = GD_p > 0. \tag{25}$$

Acting as passive circuit, at these LF, the magnitude is denoted by:

$$T(\omega \approx 0) = T_0 \leq 1 . \tag{26}$$

The NGD cut-off frequency which is the root of equation:

$$GD(\omega) = 0 \tag{27}$$

is denoted by:

$$\omega_n = 2\pi f_n . \tag{28}$$

The positive GD bandwidth is defined in the LF, $\omega < \omega_n$. Particularly to HP-NGD function, in the NGD frequency band, $\omega > \omega_n$, we have:

$$GD(\omega) < 0 \tag{29}$$

As illustrated in Fig. 4(a), the GD response of our HP-NGD response is specified by an optimal frequency, $\omega_o = 2\pi f_o$, where we have the GD minimal value:

$$\min\left[GD(\omega = \omega_o)\right] = GD_o < 0 . \tag{30}$$

As seen in Fig. 4(b), in the NGD frequency band, $\omega > \omega_n$, we can define the attenuation losses by:

$$T(\omega = \omega_n) = T_n \tag{31}$$

$$T(\omega = \omega_o) = T_o . \tag{32}$$

As concrete illustration of this unfamiliar and ideal HP-NGD function, let us consider in the following section deeper NGD analysis of circuit introduced in Fig. 1.

3.3. Frequency responses of the considered passive topology

This transmission coefficient can be identified by the canonical form:

$$T(s) = \frac{1 + \frac{a\,s}{2}}{1 + a\,s} \tag{33}$$

by taking the parameters:

$$a = R_0 C . \tag{34}$$

Substantially, the transmittance associated to our 4-port circuit defined in equation (22) is given by:

$$T(\omega) = \frac{\sqrt{1 + \frac{a^2\omega^2}{4}}}{\sqrt{1 + a^2\omega^2}} . \tag{35}$$

By definition of equation (23), the corresponding phase response is equal to:

$$\varphi(\omega) = \varphi_1(\omega) + \varphi_2(\omega) \tag{36}$$

with

$$\varphi_1(\omega) = \arctan\left(\frac{a\,\omega}{2}\right) \tag{37}$$

$$\varphi_2(\omega) = \arctan(a\,\omega)\,. \tag{38}$$

According to definition (24), the GD can be formulated as:

$$GD(\omega) = \frac{a(2-a^2\omega^2)}{(1+a^2\omega^2)(4+a^2\omega^2)}\,. \tag{39}$$

It can be understood from this expression that the circuit behaves as a HP-NGD topology.

3.4. HP-NGD characterization

The LF GD value defined in equation (25) is equal to:

$$GD_p = \frac{a}{2} = \frac{R_0 C}{2}\,. \tag{40}$$

The NGD cut-off frequency associated to equation (27) by means of expression (39) is given by:

$$f_n = \frac{1}{2\pi\sqrt{2}a} = \frac{1}{2\pi\sqrt{2}R_0 C}\,. \tag{41}$$

At the cut-off frequency, we have attenuation:

$$T_n = 1/\sqrt{2}\,. \tag{42}$$

Moreover, the optimal frequency is equal to:

$$f_o = \frac{\sqrt{3\sqrt{2}+2}}{2\pi a}\,. \tag{43}$$

It means that the ratio between the cut-off and optimal frequencies is equal to:

$$\frac{f_o}{f_n} = \sqrt{2(3+\sqrt{2})}\,. \tag{44}$$

Where the mono-capacitor circuit reaches the GD minimum which is obviously a negative quantity:

$$GD_o = \left(\frac{2\sqrt{2}}{3} - 1\right)a\,. \tag{45}$$

At this optimal frequency, the attenuation is equal to:

$$T_o = \frac{\sqrt{\sqrt{2}}}{2}\,. \tag{46}$$

The HP-NGD characteristic equation can be formulated by the NGD value and NGD cut-off frequency relationship:

$$\begin{cases} f_n GD_o = \dfrac{2\sqrt{2}-3}{6\pi\sqrt{2}} \\ f_o GD_o = \dfrac{(2\sqrt{2}-3)(\sqrt{3\sqrt{2}+2})}{6\pi} \end{cases}\,. \tag{47}$$

Fig. 5 highlights the logarithmic variation plot of the optimal GD versus the two characteristic frequencies from -1 ns to -1 ms. We can see that the two frequencies vary from 0.6436 Hz to 6.436 MHz, and 2.2742 Hz to 2.2742 MHz, respectively.

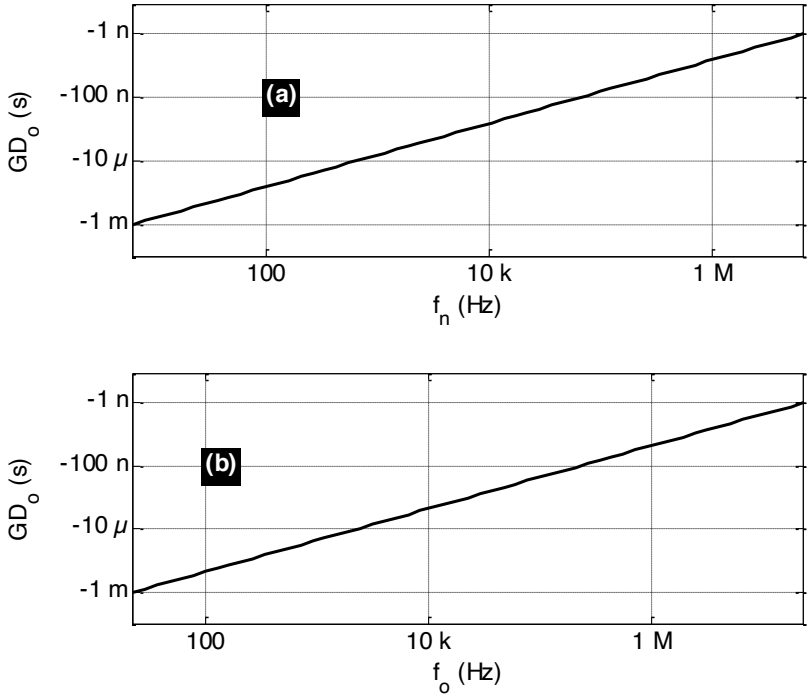

Figure 5: Variation of GD_0 versus (a) f_n and (b) f_o.

By considering a POC, the next section will be focused on the validation study of the elaborated HP-NGD circuit theory.

4. HP-NGD BEHAVIOR VALIDATIONS

The present section is focused on the mono-capacitor HP-NGD circuit validation. Doing this, the response calculated from MATLAB® will be compared with commercial tool-based S-parameter simulation.

4.1 Parametric investigation with respect to the capacitor

A general view on the GD responses of our circuit was investigated by considering the capacitor C with minimal and maximal values, C_{min}=1 pF and C_{max}=1 µF. The parametric study was performed in the frequency range swept between 1 kHz and 1 GHz. The magnitude and GD responses were computed from analytical models expressed by equation (35) and equation (38), respectively. Therefore, we obtain the computed results represented by the mappings of

reflection and transmission coefficients versus couple (frequency, capacitor) displayed by Fig. 6(a) and Fig. 6(b), respectively. We can remark that:

- The reflection coefficient magnitude, S_{11}, increases with the capacitor and frequency,
- And the transmission coefficient one, S_{21}, varies inversely.

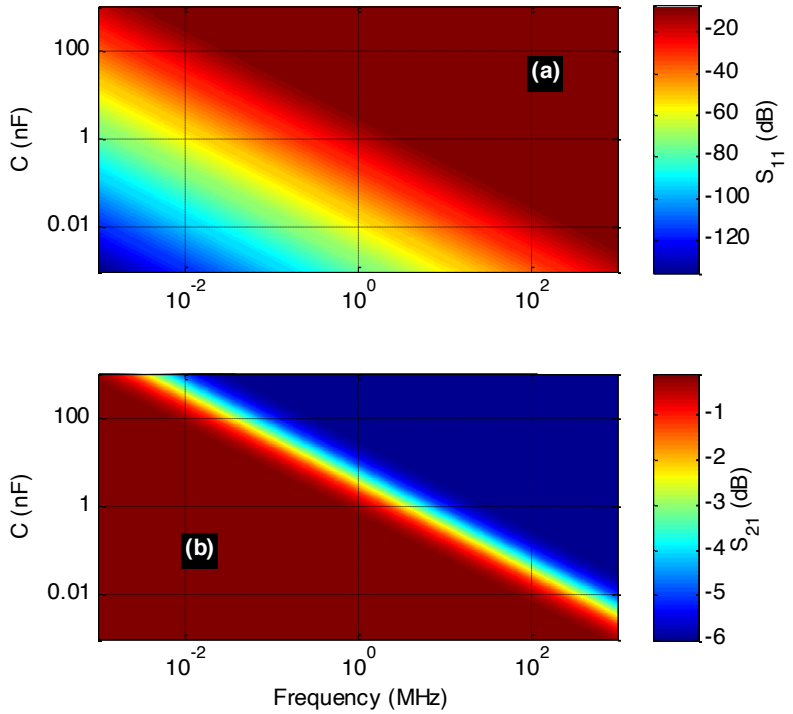

Figure 6: Mappings of (a) S_{11} and (b) S_{21} versus couple (frequency, capacitor).

More importantly, the GD response versus couple (frequency, capacitor) was also computed in the same range of variables. Figs. 7 highlight the obtained results displayed in three successive frequency bands subdivided by [1 kHz, 200 kHz], [200 kHz, 20 MHz] and [20 MHz, 1 GHz]. As shown by Fig. 7(a), the positive value of GD is located in the zone of higher value of capacitor and lower value of the frequency. Then, the NGD zone is observed when the frequency is much higher. We can understand from the three maps that the circuit is susceptible to behave as HP-NGD function with the navy-blue surface area of the mapping. Nevertheless, it can be understood that the optimal NGD frequency appears around a characteristic medium value of the capacitor. The absolute value of the NGD optimum is decreasing with the frequency.

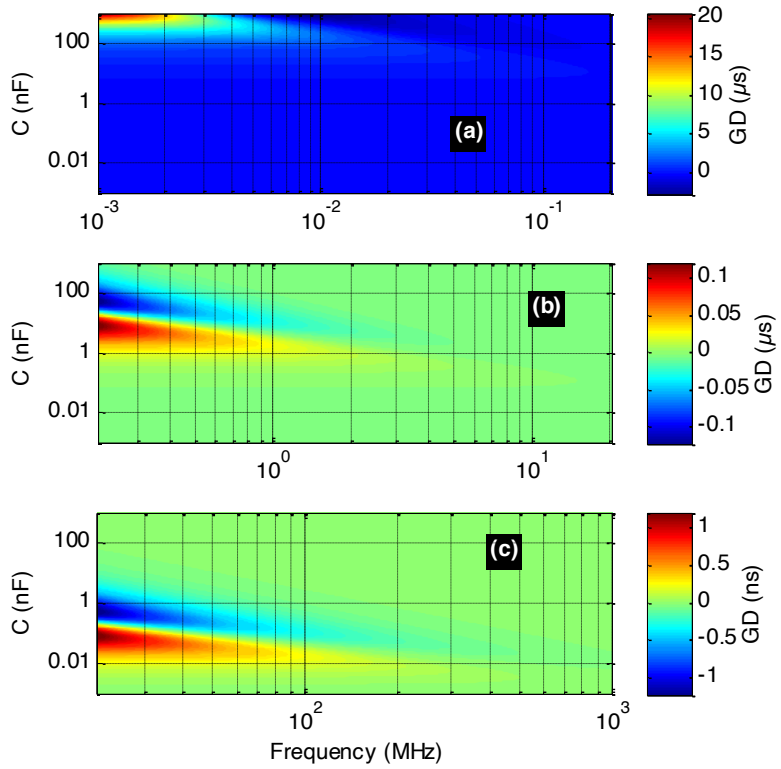

Figure 7: Mapping of GD versus couple (frequency, capacitor)
in the frequency bands, (a) [1 kHz, 200 kHz], (b) [200 kHz, 20 MHz] and (c) [20 MHz, 1 GHz].

For the better validation of the HP-NGD aspect, a comparative study between calculation and simulation was performed. The next subsection reports the POC circuit design.

4.2. Design description of the POC circuit

Our validation approach is based on the comparison between the MATLAB numerical computation of analytical expressions given in equations (35), (36) and (39) with the simulation results from the commercial tool of electronic circuit simulator "Advanced Design System (ADS®)" from Keysight Technologies®. The schematic design of the mono-capacitor circuit designed in the ADS® environment is illustrated by Fig. 8. It acts as a four-port circuit with terminals operating under reference impedance R_0=50 Ω. A lumped capacitor with nominal value C=22 pF was considered as an arbitrary test component.

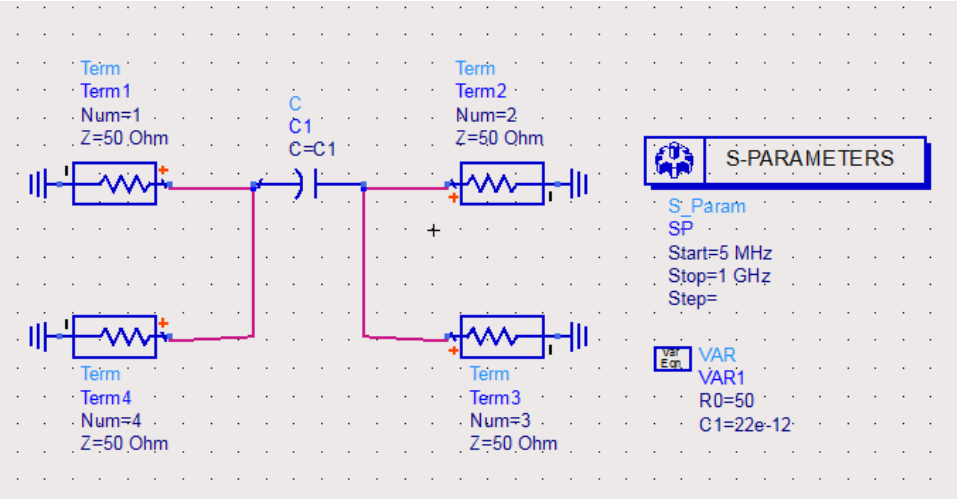

Figure 8: ADS® design of the simulated NGD passive mono-capacitor 4-port circuit.

The S-parameter simulation of the circuit was carried out in the frequency band delimited by 5 MHz and 1 GHz. After ADS® simulation, we obtain the results discussed in the next subsection.

4.3. Comparative study of calculated and simulated HP-NGD responses

First and foremost, as the main target of the applicative study, the NGD specifications expected for our POC circuit are indicated in following Table 2. To observe obviously the BP NGD behavior, the present applicative study is performed in AC regime withing the frequency range 100 kHz and 150 kHz. Substantially, the compared calculated and simulated frequency responses of the POC RLCP circuit are plotted in Fig. 5. It can be observed that the magnitude, phase and GD shown in Fig. 5(a), Fig. 5(b) and Fig. 5(c), respectively are in excellent agreement. It is validated undeniably with Fig. 5(c) that the RLCP circuit presents a BP NGD function behavior. It is noteworthy that the discrepancies between the calculations and simulations are insignificant in the whole considered working frequency range. Moreover, the comparisons between the NGD performance parameters are addressed in Table 3. As reported in this recapitulative table, the calculation and simulation differences are almost zero (indeed zero for frequency). This fully agrees with the behavior of resonant circuits, for which the phase corresponding to the NGD center frequency is equal to zero.

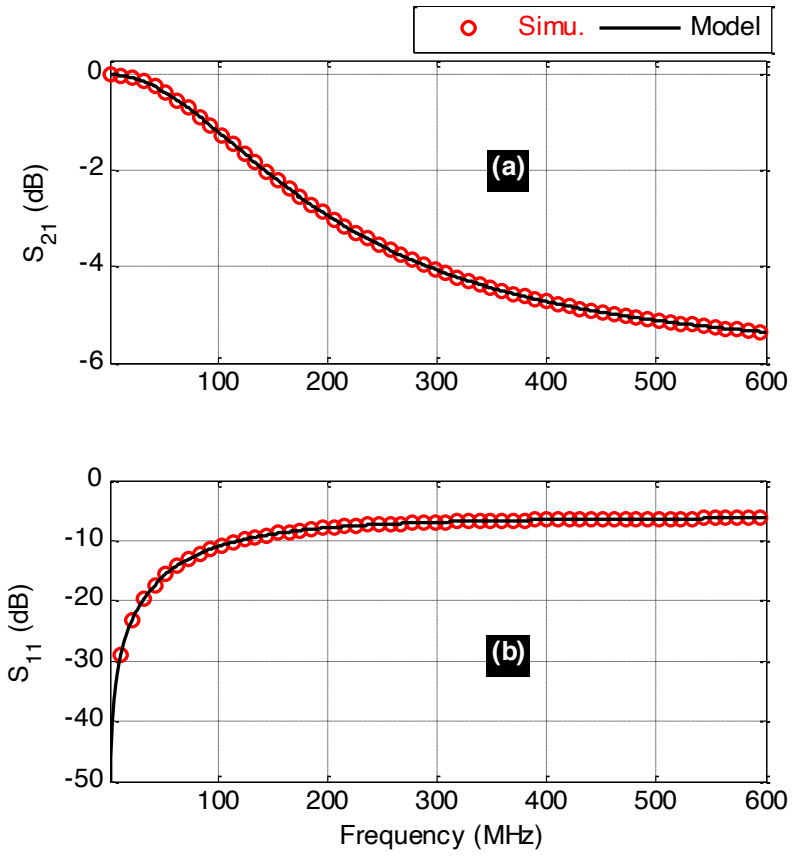

Figure 9: Comparison between the calculated and simulated (a) S_{11} and (b) S_{21} magnitudes of the POC HP-NGD circuit shown in Fig. 8.

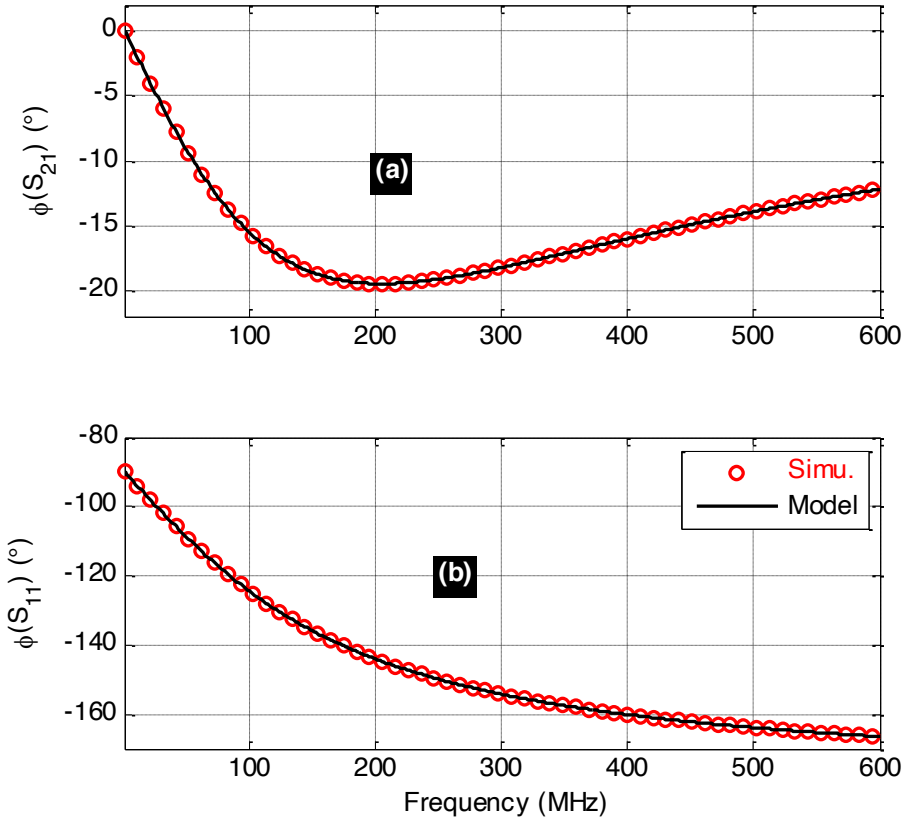

Figure 10: Comparison between calculated and simulated (a) S_{11} and (b) S_{21} phases of the POC circuit shown in Fig. 4.

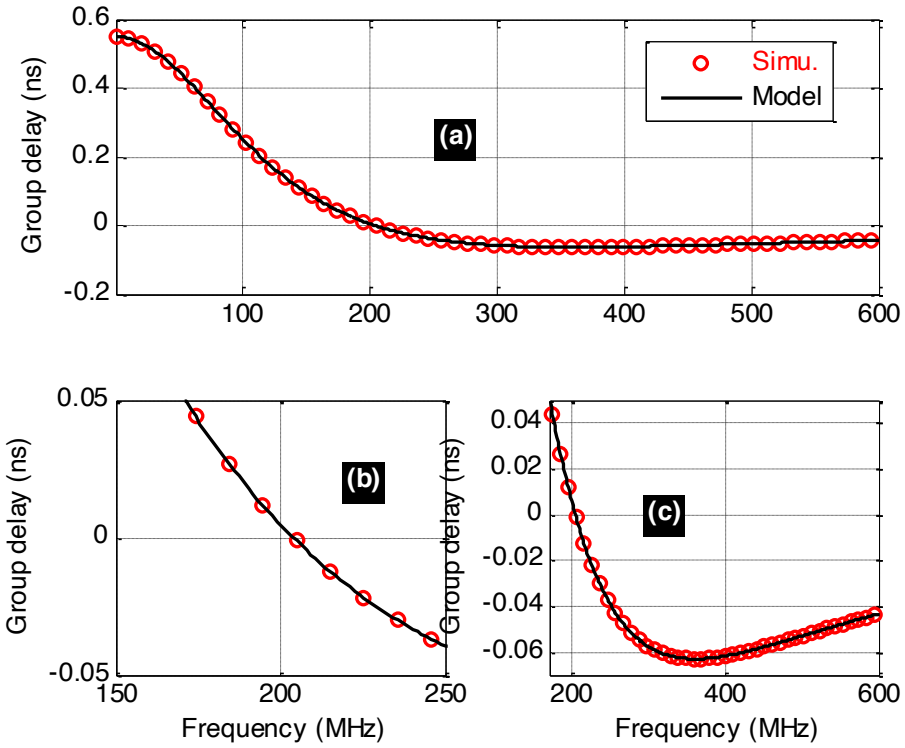

Figure 11: Comparison between calculated and simulated GD of the POC circuit shown in Fig. 8 in the frequency bands (a) [1 Hz, 600 MHz], (b) [150 MHz, 250 MHz] and (c) [170 MHz, 600 MHz].

Parameters	f_n	f_{c1}	f_{c2}	BW_{NGD}	GD_n	*FoM*
Values	125 kHz	120 kHz	130.1 kHz	10 kHz	-36.79 µs	0.1225

Table 2: *Targeted NGD specifications*

Approach	f_n (kHz)	f_{c1} (kHz)	f_{c2} (kHz)	*BW* (kHz)	T_n (dB)	GD_n (µs)	*FoM*
Calc.	125	120.1	130.09	9.9901	-9.5424	-36.792	0.12252
Simu.	125	120.1	130.1	10	-9.541	-36.78	0.1225
Gap (%)	0	0	0.0077	0.0991	0.32	0.0326	0.0163

Table 3: *Comparison between the calculated and simulated NGD parameters*

The NGD phenomenon appears explicitly at the center frequency with NGD value of about GD_n=-37 µs over the NGD bandwidth, BW_n=10 kHz. In other words, this bandwidth corresponds to about 8% of the NGD center frequency. The RLCP circuit attenuation is of about 9.54 dB at the NGD center frequency. We can point out that this result satisfies the condition for maximizing the FoM as earlier predicted in Fig. 2. After this spectacular validation results, we are wondering about a curious question ever being answered in the previous NGD investigation available in the literature

[7-35] about the influence of the R, L and C component tolerances on the NGD performances. The answer to this question constitutes the main object of the following section.

6. CONCLUSION

An original circuit theory on the HP-NGD four-port typical H-shape topology ever being done before is developed. The considered topology is essentially comprised of a single mono-capacitor.

The S-parameter model of the mono-capacitor topology is established from the admittance matrix expression. The theoretical development of the HP-NGD analytical approach is elaborated. An innovative characterization of the HP-NGD specifications in function of the *C* component value is introduced. The main specifications of the HP-NGD function as the NGD cut-off frequency, NGD optimal frequency and optimal NGD value, and attenuation were investigated in function of frequency variations and the capacitor element. The analytical expressions of each NGD specification were established. To validate the HP-NGD theory, results of from analytical and simulation with the ADS® commercial tool were discussed. It was demonstrated from parametric analyses that the four-port topology is susceptible to behave as an HP-NGD function. Moreover, calculated and simulated results in very good correlation are obtained.

In the future, we expect expanded applications of HP-NGD circuits with higher number of port topology. In this optics, the present NGD investigation approach could contribute to the processing of transmission signals requiring optimization in terms of transmission delay.

REFERENCES

[1] G. Groenewold, “Noise and group delay in active filters,” IEEE Trans. Circuits Syst. Regul. Pap., vol. 54, no. 7, pp. 1471-1480, 2007.

[2] S.-S. Myoung, B.-S. Kwon, Y.-H. Kim, et J.-G. Yook, “Effect of group delay in RF BPF on impulse radio systems,” IEICE Trans. Commun., vol. 90, no. 12, pp. 3514-3522, 2007.

[3] G. Agrawal, S. Aniruddhan, et R. K. Ganti, “Multi-band RF time delay element based on frequency translation,” in 2014 IEEE International Symposium on Circuits and Systems (ISCAS), Melbourne, VIC, Australia, 1-5 June 2014, pp. 1368-1371.

[4] J. -K. Xiao, Q. -F. Wang and J. -G. Ma, "Negative Group Delay Circuits and Applications: Feedforward Amplifiers, Phased-Array Antennas, Constant Phase Shifters, Non-Foster Elements, Interconnection Equalization, and Power Dividers," IEEE Microwave Magazine, vol. 22, no. 2, pp. 16-32, Feb. 2021.

[5] B. Ravelo, “Neutralization of LC- and RC-Effects with Left-Handed and NGD Circuits”, Advanced Electromagnetics (AEM), Vol. 2, No. 1, Sept. 2013, pp. 73-84.

[6] Ravelo, B., Rahajandraibe, W., Gan, Y., Wan, F., Murad N. M., Douyère, A. “Reconstruction Technique of Distorted Sensor Signals with Low-Pass NGD Function,” IEEE Access, vol. 8, no. 1, pp. 92182-92195, 2020.

[7] C. D. Broomfield and J. K. A. Everard, “Broadband Negative Group Delay Networks for Compensation of Oscillators, Filters and Communication Systems,” Electron. Lett., Vol. 36, No. 23, pp. 1931-1933, Nov. 2000.

[8] H. Choi, Y. Jeong, C. D. Kim, and J. S. Kenney, “Efficiency enhancement of feedforward amplifiers by employing a negative group delay circuit,” IEEE Trans. Microw. Theory Tech., Vol. 58, No. 5, May 2010, pp. 1116–1125.

[9] H. Choi, Y. Jeong, C. D. Kim, and J. S. Kenney, “Bandwidth enhancement of an analog feedback amplifier by employing a negative group delay circuit,” Progress In Electromagnetics Research, Vol. 105, 2010, pp. 253-272.

[10] M. Zhu and C.-T. M. Wu, “Reconfigurable Series Feed Network for Squint-free Antenna Beamforming Using Distributed Amplifier-Based Negative Group Delay Circuit,” in Proc. 2019 49th European Microwave Conference (EuMC), Paris, France, 1-3 Oct. 2019, pp. 256-259.

[11] S. Chu and S. Wong, “Linear Pulse Propagation in an Absorbing Medium,” Phys. Rev. Lett., Vol. 48, 1982, pp. 738-741.

[12] B. Ségard and B. Macke, “Observation of Negative Velocity Pulse Propagation,” Phys. Lett. A, Vol. 109, 1985, pp. 213-216.

[13] J. N. Munday and W. M. Robertson, “Observation of Negative Group Delays within a Coaxial Photonic Crystal Using an Impulse Response Method,” Optics Communications, Vol. 273, No. 1, 2007, pp. 32-36.

[14] B. Ségard and B. Macke, “Two-pulse interference and superluminality,” Optics Communications, Vol. 281, No. Jan. 2008, pp. 12–17.

[15] M. W. Mitchell, and R. Y. Chiao, “Negative group delay and "fronts" in a causal system: An experiment with very low frequency bandpass amplifiers,” Phys. Lett. A, vol. 230, no. 3-4, June 1997, pp. 133-138.

[16] M. W. Mitchell and R.Y. Chiao, “Causality and Negative Group-delays in a Simple Bandpass Amplifier,” Am. J. Phys., vol. 66, 1998, pp. 14-19.

[17] T. Nakanishi, K. Sugiyama and M. Kitano, “Demonstration of Negative Group-delays in a Simple Electronic Circuit,” Am. J. Phys., vol. 70, no. 11, 2002, pp. 1117-1121.

[18] M. Kitano, T. Nakanishi and K. Sugiyama, “Negative Group-delay and Superluminal Propagation: An Electronic Circuit Approach,” IEEE J. Sel. Top. in Quantum Electron., vol. 9, no. 1, Feb. 2003, pp. 43-51.

[19] J. N. Munday and R. H. Henderson, “Superluminal Time Advance of a Complex Audio Signal,” Appl. Phys. Lett., vol. 85, no. 3, July 2004, pp. 503-504.

[20] M. Kandic and G. E. Bridges, “Asymptotic Limits of Negative Group Delay in Active Resonator-Based Distributed Circuits,” IEEE Transactions on Circuits and Systems I: Regular Papers, Vol. 58, No. 8, Aug. 2011, pp. 1727-1735.

[21] G. V. Eleftheriades, O. Siddiqui, and A. K. Iyer, “Transmission Line for Negative Refractive Index Media and Associated Implementations without Excess Resonators,” IEEE Microw. Wireless Compon. Lett., Vol. 13, No. 2, pp. 51-53, Feb. 2003.

[22] O. F. Siddiqui, M. Mojahedi and G. V. Eleftheriades, “Periodically Loaded Transmission Line With Effective Negative Refractive Index and Negative Group Velocity,” IEEE Trans. Antennas Propagat., Vol. 51, No. 10, Oct. 2003, pp. 2619-2625.

[23] L. Markley and G. V. Eleftheriades, “Quad-Band Negative-Refractive-Index Transmission-Line Unit Cell with Reduced Group Delay,” Electronics Letters, Vol. 46, No. 17, Aug. 2010, pp. 1206-1208.

[24] G. Monti and L. Tarricone, “Negative Group Velocity in a Split Ring Resonator-Coupled Microstrip Line,” Progress In Electromagnetics Research, Vol. 94, pp. 33-47, 2009.

[25] G. Liu, and J. Xu, “Compact transmission-type negative group delay circuit with low attenuation,” Electronics Letters, Vol. 53, No. 7, Mar. 2017, pp. 476-478.

[26] G. Chaudhary, and Y. Jeong, “Tunable center frequency negative group delay filter using coupling matrix approach,” IEEE Microwave Wireless Component Letters, Vol. 27, No. 1, 2017, pp. 37-39.

[27] T. Shao, S. Fang, Z. Wang and H. Liu, “A Compact Dual-Band Negative Group Delay Microwave Circuit,” Radio Engineering, vol. 27, no. 4, pp. 1070-1076, Dec. 2018.

[28] C.-T. M. Wu and T. Itoh, “Maximally Flat Negative Group Delay Circuit: A Microwave Transversal Filter Approach,” IEEE Trans. on Microwave Theory and Techniques, Vol. 62, No. 6, June 2014, pp. 1330-1342.

[29] T. Zhang, R. Xu and C. M. Wu, “Unconditionally Stable Non-Foster Element Using Active Transversal-Filter-Based Negative Group Delay Circuit,” IEEE Microw. Wireless Compon. Lett., vol. 27, no. 10, pp. 921-923, Oct. 2017.

[30] B. Ravelo, “Synthesis of RF Circuits with Negative Time Delay by Using LNA”, Advanced Electromagnetics (AEM), Vol. 2, No. 1, Feb. 2013, pp. 44-54.

[31] B. Ravelo, “Similitude between the NGD function and filter gain behaviours,” Int. J. Circ. Theor. Appl., Vol. 42, No. 10, Oct. 2014, pp. 1016-1032.

[32] B. Ravelo, F. Wan, J. Nebhen, G. Chan, W. Rahajandraibe and S. Lalléchère, “Bandpass NGD TAN of Symmetric H-Tree with Resistorless Lumped-Network,” IEEE Access, Vol. 9, pp. 41383-41396, Mar. 2021.

[33] F. Wan, Y. Liu, J. Nebhen, Z. Xu, G. Chan, S. Lalléchère, R. Vauche, W. Rahajandraibe and B. Ravelo, “Bandpass Negative Group Delay Theory of Fully Capacitive Δ-Network,” IEEE Access, Vol. 9, No. 1, pp. 62430 - 62445, Apr. 2021.